MATERIALE PLASTICE
https://revmaterialeplastice.ro
https://doi.org/10.37358/Mat.Plast.1964

CC BY

Localized Drug Delivery Using Biodegradable Poly(lactic-co-glycolic acid) Microspheres: *In Vitro* Evaluation in Non-Small Cell Lung Cancer Models

LIN SHEN[1]*, FANZHI MEN[2], CHANGCHANG HU[1], BIN QIAO[3]
[1] Marketing Department, Anhui Nutrition Biotechnology Co., Ltd., Hefei, China
[2] Department of Pharmacy, Huaibei People's Hospital, Huaibei, China
[3] Department of Immunology, Fudan University, Shanghai, China

Abstract: ***Background:*** *Non-small cell lung cancer has a high risk of local recurrence after surgery, and localized sustained drug delivery is of interest for improving local drug exposure. Poly(lactic-co-glycolic acid) microspheres are promising carriers due to their biodegradability and controllable release behavior.* ***Methods:*** *Doxorubicin-loaded poly(lactic-co-glycolic acid) microspheres were prepared and characterized by scanning electron microscopy and dynamic light scattering. Encapsulation efficiency, drug loading, release behavior, and in vitro biological responses were evaluated.* ***Results:*** *The microspheres were predominantly spherical, with an average hydrodynamic diameter of about 200 nm. Encapsulation efficiency and drug loading were approximately 80% and 7%, respectively. Cumulative release reached about 60% in PBS and 75–80% under reactive oxygen species-containing conditions after 72 h. Blank microspheres maintained cell viability above 95%, whereas the loaded formulation reduced viability to about 60% at 72 h and 55–58% after prolonged incubation.* ***Conclusion:*** *These findings suggest that poly(lactic-co-glycolic acid) microspheres provide a feasible in vitro platform for localized and sustained doxorubicin delivery, although further validation in more physiologically relevant models is still required.*

Keywords: *Non-small cell lung cancer, 2D and 3D cell models, biodegradable poly, microspheres*

1. Introduction

Non-small cell lung cancer (NSCLC) is the predominant form of lung cancer [1]. Lung cancer was the leading cause of cancer-related death worldwide in 2022, accounting for an estimated 1.8 million deaths [2]. Positive surgical margins after NSCLC resection can leave residual disease and increase the risk of recurrence [3]. A national cohort study of early-stage lung cancer associated positive margins with poorer survival after resection [4]. Adjuvant vinorelbine plus cisplatin improved survival after complete resection of early-stage NSCLC, although treatment-related toxicity was observed [5]. In a murine NSCLC resection model, locally implanted paclitaxel-releasing polymer films increased drug exposure at the surgical site and reduced local recurrence [6]. Paclitaxel-loaded PLGA microspheres also inhibited lung carcinoma growth in a mouse model of microscopic malignant disease, supporting a preclinical rationale for local delivery [7]. Drug-loaded PLGA-PEG microspheres implanted after tumor resection improved outcomes in a mouse model of triple-negative breast cancer [8]. These findings motivate the investigation of localized, sustained-release drug delivery; however, evidence from other formulations and tumor models does not establish efficacy for postoperative NSCLC treatment.

Biodegradable polymeric microspheres, particularly those based on poly(lactic-co-glycolic acid) (PLGA), have attracted attention as controlled-release drug carriers because of their biodegradability and established use in biomedical products [9]. From a materials perspective, the lactic acid/glycolic acid ratio, molecular weight, and end-group chemistry influence PLGA degradation and drug release [9].

email: shenlinss@163.com

Drug release from PLGA-based systems can involve diffusion, polymer degradation, erosion, and swelling [10]. Doxorubicin (DOX) has been encapsulated in PLGA-based microparticles and evaluated for release behavior and cytotoxicity in glioma C6 cells [11]. Electrosprayed DOX-loaded PLGA microspheres have also been investigated for sustained delivery and potential intratumoral injection [12]. Studies of PLGA microsphere/PVA hydrogel composites have linked water uptake and internal pore formation to drug release [13]. In double-walled PDLLA(PLGA) microspheres, the polymer configuration influences the mechanism of drug release [14]. Formulation and processing parameters also affect the size of PLGA microparticles produced by emulsion methods [15]. For local antitumor delivery, docetaxel-loaded PLGA microparticles inhibited tumor growth after peritumoral injection in a prostate cancer xenograft model [16]. Paclitaxel microspheres incorporated into an *in situ* gel delayed postoperative recurrence in a 4T1 tumor model [17]. In lung cancer, intrapleural placement of a gelatin sponge containing PLGA-paclitaxel microspheres was investigated for regional drug delivery and control of lymphatic metastasis [18]. These studies provide formulation-specific precedents for local chemotherapy. Further investigation is needed to determine how a DOX-loaded PLGA formulation performs under defined release conditions and in NSCLC cell models before considering postoperative application.

Drug penetration and response in 3D tumor spheroids are influenced by compact multicellular organization and transport barriers [19]. Sustained delivery of DOX and paclitaxel from hollow PLGA microparticles has been evaluated in MCF-7 tumor spheroids [20]. Therefore, a delivery system capable of maintaining drug availability over time may provide an advantage over transient bolus exposure. PLGA was selected because it can serve as a biodegradable carrier for controlled drug release, which may prolong DOX exposure in the spheroid microenvironment. We hypothesized that this sustained-release profile would enhance drug action in 3D tumor spheroids and thereby lead to stronger cytotoxic effects compared with free DOX treatment. In this study, we developed DOX-loaded PLGA microspheres as an *in vitro* platform for evaluating sustained local drug delivery. The physicochemical properties, drug loading efficiency, and release kinetics of the microspheres were systematically evaluated. *In vitro* cytocompatibility, hemocompatibility, and antitumor responses were assessed using 2D and 3D NSCLC cell models. Furthermore, a conceptual framework was proposed to illustrate the potential use of a local microsphere depot near a resection margin. This work aims to inform future studies of postoperative local chemotherapy for NSCLC; implantation, postoperative recurrence, and therapeutic efficacy *in vivo* were not evaluated in the present study.

2. Materials and methods

2.1. Materials

Poly(lactic-co-glycolic acid) (PLGA, lactide:glycolide = 50:50, Mw ≈ 30,000–60,000) and poly(vinyl alcohol) (PVA, 87–89% hydrolyzed, Mw ≈ 30,000–70,000) were purchased from Sigma-Aldrich (St. Louis, MO, USA). Doxorubicin hydrochloride (DOX·HCl) was obtained from Aladdin (Shanghai, China). Citrated sheep blood was purchased from Shanghai Yuanye Bio-Technology Co., Ltd., Shanghai, China. Dichloromethane (DCM), dimethyl sulfoxide (DMSO), and phosphate-buffered saline (PBS, pH 7.4) (Shanghai Yuanye Bio-Technology Co., Ltd., Shanghai, China) were analytical grade and used without further purification. Calcein-AM and Ethidium homodimer-1 (EthD-1) were purchased from Thermo Fisher Scientific (Waltham, MA, USA) for live/dead staining. Human non-small cell lung cancer cell lines A549 and H1299 were supplied by the Chinese Academy of Sciences Cell Bank (Shanghai, China) and cultured in DMEM (Gibco, Grand Island, NY, USA) supplemented with 10% fetal bovine serum (FBS) (Shanghai Yuanye Bio-Technology Co., Ltd., Shanghai, China) and 1% penicillin–streptomycin (Shanghai Yuanye Bio-Technology Co., Ltd., Shanghai, China) under 37°C and 5% CO_2. Esterase, reduced glutathione (GSH), physiological saline, 2′,7′-dichlorodihydrofluorescein diacetate (DCFH-DA), N-acetyl-L-cysteine (NAC), hydrogen peroxide (H_2O_2), deionized water, and

ultra-low-attachment 96-well plates were purchased from Shanghai Yuanye Bio-Technology Co., Ltd. (Shanghai, China). Cell Counting Kit-8 (CCK-8) was obtained from Dojindo (Mashiki, Japan).

2.2. Preparation of DOX-loaded PLGA microspheres

Drug-loaded microspheres were fabricated using a water-in-oil-in-water (W/O/W) double-emulsion solvent evaporation method. Briefly, 20 mg of DOX·HCl was dissolved in 1 mL of deionized water and added dropwise into 4 mL of DCM containing 200 mg of PLGA under sonication (Ultrasonic processor, 30 W, 20 s) to form the primary W/O emulsion. The primary emulsion was immediately poured into 50 mL of 1% (w/v) PVA aqueous solution and homogenized at 12,000 rpm for 2 min to form the secondary W/O/W emulsion. The emulsion was stirred magnetically at room temperature for 4 h to allow solvent evaporation. The resulting microspheres were collected by centrifugation (8000 rpm, 10 min), washed three times with deionized water, and lyophilized for 48 h. Blank PLGA microspheres were prepared using the same procedure without DOX.

2.3. Morphological and size characterization

The surface morphology of dried microspheres was observed using scanning electron microscopy (SEM, Hitachi SU8010, Tokyo, Japan) after sputter-coating with gold. The average particle size and polydispersity index (PDI) were determined by dynamic light scattering (DLS, Malvern Zetasizer Nano ZS, Malvern, UK) using samples dispersed in deionized water at 25°C. All measurements were performed in triplicate.

2.4. Drug loading and encapsulation efficiency

Encapsulation efficiency (EE%) and drug loading (DL%) were determined by dissolving 10 mg of microspheres in 2 mL of DMSO and measuring DOX absorbance at 480 nm using a UV–Vis spectrophotometer (Thermo Evolution 300). Encapsulation efficiency was defined as the percentage of encapsulated DOX relative to the initial amount of DOX added during preparation, while drug loading was defined as the percentage of encapsulated DOX relative to the total mass of microspheres. Each test was conducted in triplicate, and mean ± SD values were reported.

2.5. *In vitro* drug release

For release studies, 10 mg of DOX-loaded microspheres were suspended in 10 mL of PBS (pH 7.4, 6.5, or PBS + esterase 10 U/mL; reducing condition: PBS + 5 mM GSH) and incubated at 37°C under gentle shaking (100 rpm). At predetermined intervals, 1 mL of supernatant was withdrawn and replaced with fresh medium. The cumulative release was quantified by UV–Vis at 480 nm.

2.6. Cytocompatibility and cytotoxicity assays

A549 and H1299 cells were seeded in 96-well plates (5×10^3 cells/well) and incubated overnight. The medium was replaced with extracts of blank or DOX-loaded microspheres (10 mg/mL equivalent) prepared by immersing microspheres in culture medium for 24 h at 37°C. After incubation for 24–168 h, cell viability was evaluated using the CCK-8 assay (Dojindo, Mashiki, Japan). Absorbance at 450 nm was measured using a microplate reader (BioTek Synergy HTX), and cell viability was expressed as the percentage relative to untreated controls.

2.7. Hemolysis test

Sheep red blood cells (RBCs) were isolated from the citrated sheep blood by centrifugation and washed with physiological saline until the supernatant became clear. Microspheres (10 mg/mL) were incubated with 2% sheep RBC suspension at 37°C for 3 h. After centrifugation at 1500 rpm for 10 min, the absorbance of the supernatant was measured at 540 nm. Saline and deionized water were used as the negative and positive controls, respectively. The hemolysis ratio was calculated as Hemolysis (%) = [(A_sample − A_negative)/(A_positive − A_negative)] × 100, where *A_sample*,

A_negative, and *A_positive* represent the absorbance values of the sample, negative control, and positive control, respectively.

2.8. 3D tumor spheroid culture and live/dead staining

For 3D models, A549 cells were seeded in ultra-low-attachment 96-well plates (5×10^3 cells/well) and cultured for 5 days to form compact spheroids. Microsphere extracts (blank or DOX-loaded) were then added and incubated for 7 days. Spheroids were stained with Calcein-AM (2 μM) and EthD-1 (4 μM) for 30 min at 37°C in the dark, followed by imaging under a confocal fluorescence microscope (Leica TCS SP8, Wetzlar, Germany). Spheroid volume was estimated from diameter measurements using ImageJ. Intracellular ROS generation in A549 tumor spheroids was measured using DCFH-DA staining. After spheroid formation, the spheroids were treated with control medium, blank PLGA microspheres, free DOX, DOX-loaded PLGA microspheres, or DOX-loaded PLGA microspheres in the presence of NAC (5 mM) for 72 h. The DOX concentration in the free DOX group was matched to the DOX-equivalent concentration in the DOX-loaded PLGA microsphere group, and the blank PLGA group was matched to the polymer amount used in the DOX-loaded PLGA group. After treatment, spheroids were washed with PBS and incubated with DCFH-DA (10 μM) for 30 min at 37°C in the dark. Fluorescence images were acquired under identical imaging settings, and the mean fluorescence intensity was quantified using ImageJ. ROS levels were normalized to the untreated control group and presented as mean ± SD from three independent replicates.

2.9. Statistical analysis

All experiments were conducted in triplicate, and data are presented as mean ± SD. Statistical comparisons were performed using one-way ANOVA with Tukey's post-hoc test (GraphPad Prism 9.0). A p-value < 0.05 was considered statistically significant.

2.10. AI tools

DeepSeek was used solely for language polishing and minor editorial refinement of the manuscript, including improving grammar, readability, and sentence structure.

3. Results

Figure 1 presents the overall design concept and experimental rationale of this study. DOX-loaded PLGA microspheres were designed as a biodegradable local drug depot to prolong drug exposure in a postoperative treatment-mimicking setting. In this model, microspheres implanted near residual tumor cells at the resection margin would gradually release DOX, thereby reducing the need for transient bolus administration and maintaining local drug availability over time. The schematic also defines the *in vitro* evaluation strategy used in the present work. A 3D NSCLC tumor spheroid model was used to mimic key features of residual tumor cell clusters, including compact cell packing and diffusion barriers. DOX-loaded PLGA microspheres were therefore evaluated not only for their release behavior but also for their ability to induce cytotoxic responses in tumor spheroids. This integrated design links material performance, sustained DOX delivery, and tumor-cell inhibition within a single experimental framework.

As shown in Figure 2A, the prepared PLGA microspheres exhibited a predominantly spherical morphology with relatively rough surfaces. A small degree of particle aggregation was observed; however, individual microspheres remained clearly distinguishable without evidence of fusion or collapse. The overall particle size observed by SEM was on the submicron scale, indicating that the emulsion-based fabrication process produced structurally intact microspheres. The hydrodynamic size distribution of the microspheres was further evaluated by DLS (Figure 2B). The intensity-weighted profile revealed a bimodal distribution, with a major population centered at approximately 80–100 nm and a secondary peak around 250–300 nm. The average hydrodynamic diameter was approximately 130 nm, accompanied by a moderate polydispersity index, suggesting a relatively broad but acceptable

size distribution for PLGA microspheres prepared via double-emulsion methods. To assess the responsiveness of the microspheres to oxidative environments, molecular weight retention was monitored under different incubation conditions (Figure 2C). In PBS (pH 7.4), the PLGA microspheres exhibited a gradual decrease in molecular weight, retaining approximately 88% of their initial Mw after 168 h. In contrast, microspheres exposed to ROS-containing medium showed a markedly accelerated decrease in Mw, with retention dropping to approximately 60% over the same period, indicating enhanced degradation under oxidative conditions. The colloidal stability of the microspheres in biologically relevant media was examined by tracking changes in hydrodynamic diameter and PDI in serum-containing culture medium (Figure 2D). Over 48 h of incubation, the average particle size increased moderately from approximately 135 to 165 nm, accompanied by a gradual increase in PDI. No abrupt size changes or severe aggregation were detected, suggesting that the microspheres maintained acceptable dispersion stability under cell culture conditions.

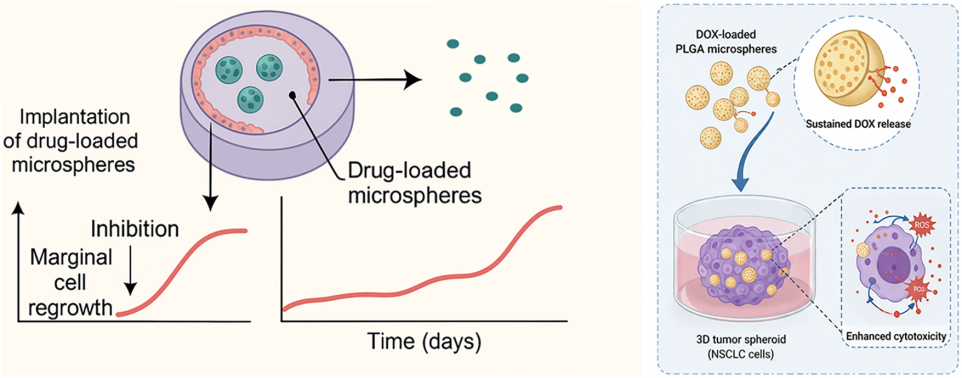

Figure 1. Conceptual framework for localized DOX delivery using PLGA microspheres in NSCLC models. The schematic illustrates the proposed use of drug-loaded PLGA microspheres as a local depot for postoperative treatment-mimicking conditions. After implantation near the tumor resection margin, the microspheres are expected to provide sustained DOX release over time, thereby maintaining local drug exposure and suppressing residual marginal cell regrowth. The right panel summarizes the *in vitro* 3D NSCLC tumor spheroid model used to evaluate DOX-loaded PLGA microspheres, including sustained drug release, microsphere–spheroid interaction, and enhanced cytotoxic responses. ROS-related cellular stress is shown as a putative DOX-associated mechanism and should be interpreted as a schematic hypothesis rather than direct quantitative evidence unless supported by additional ROS assays

As shown in Figure 2A, the PLGA microspheres achieved an encapsulation efficiency of approximately 80% with a drug loading content around 7%, indicating that the preparation process enabled efficient incorporation of the payload into the polymer matrix without substantial loss during emulsification and solvent removal. Figure 3 presents the time-dependent cumulative release profiles under different incubation conditions. In PBS (pH 7.4), release proceeded gradually and approached roughly 55–60% at 72 h, suggesting a sustained release behavior dominated by diffusion through the polymer matrix and slow polymer erosion. In mildly acidic medium (pH 6.5), the cumulative release increased relative to neutral PBS, reaching approximately 70% at 72 h. Under ROS-containing conditions, the release rate was further accelerated, with cumulative release rising to approximately 75–80% by 72 h, demonstrating a clear environment-dependent modulation of release kinetics. Figure 3 illustrates the time-dependent cytocompatibility and hemocompatibility profiles of the PLGA microspheres. Cells treated with extracts from blank microspheres consistently maintained high viability throughout the entire observation period, with viability values remaining above 95% even after extended incubation. This result indicates that neither the PLGA matrix nor potential residual components from the fabrication

process induced detectable cytotoxic effects under the tested conditions. In contrast, cells exposed to extracts from payload-loaded microspheres exhibited a gradual and progressive decrease in viability as incubation time increased. Cell viability declined from approximately 95% at early time points to around 60% after prolonged exposure, reflecting cumulative cellular response to the released payload rather than abrupt toxicity. Notably, no sharp drop in viability was observed at early time points, suggesting the absence of an initial burst release. In parallel, hemolysis assays demonstrated that both blank and loaded microspheres induced minimal red blood cell damage. The hemolysis ratios of blank microspheres remained below 1.5% at all time points, while the payload-loaded microspheres showed slightly elevated but still low hemolysis levels, consistently below 2%. These values fall well within the generally accepted range for hemocompatible materials, indicating that the microspheres did not significantly compromise erythrocyte membrane integrity.

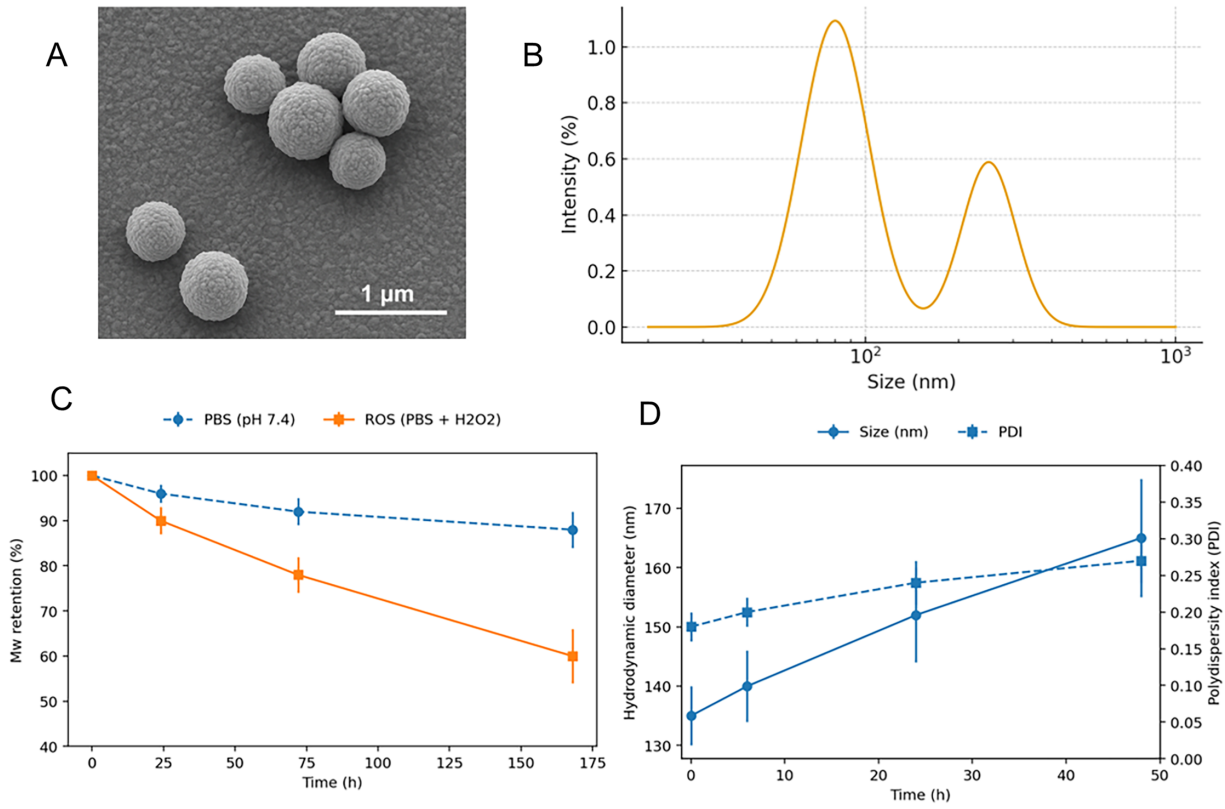

Figure 2. Morphological characterization, size distribution, ROS-triggered degradation, and colloidal stability of PLGA microspheres. (**A**) Representative SEM image showing the surface morphology and aggregation state of PLGA microspheres. (**B**) Dynamic light scattering (DLS) intensity-weighted size distribution of the microspheres. (**C**) Molecular weight (Mw) retention of PLGA microspheres incubated in PBS (pH 7.4) or ROS-containing medium (PBS supplemented with H_2O_2) over time. (**D**) Changes in hydrodynamic diameter and polydispersity index (PDI) of PLGA microspheres during incubation in serum-containing culture medium. Data are presented as mean ± SD (n = 3)

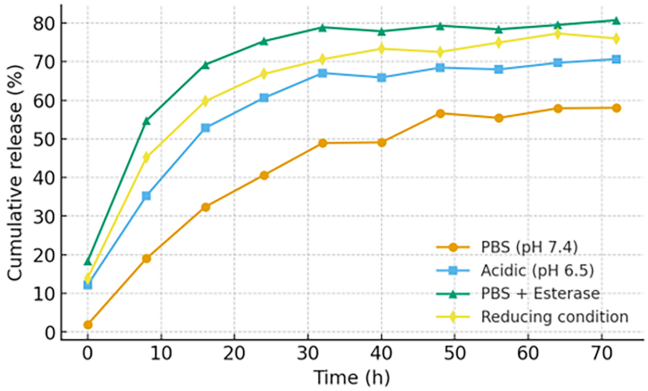

Figure 3. Cumulative release behavior of PLGA microspheres under different environments. Cumulative release profiles measured in PBS (pH 7.4), mildly acidic medium (pH 6.5), and ROS-containing medium (PBS supplemented with H_2O_2) over 72 h. Data are shown as mean ± SD (n = 3)

Figure 4 presents the long-term cell viability profiles of A549 and H1299 cells following exposure to extracts from blank and payload-loaded PLGA microspheres. For both cell lines, treatment with blank microsphere extracts resulted in consistently high viability throughout the entire 168 h incubation period, with viability remaining above 95%, indicating that prolonged exposure to the PLGA carrier did not induce delayed cytotoxic effects. In contrast, cells treated with extracts from payload-loaded microspheres exhibited a clear time-dependent decline in viability. For A549 cells, viability decreased progressively from approximately 90% at 72 h to around 55% at 168 h, while H1299 cells showed a similar trend, with viability declining from approximately 92% to about 58% over the same period. Importantly, the decrease in viability occurred gradually over time, without abrupt drops at early time points, suggesting that the observed cellular response reflects cumulative exposure to the released payload rather than acute toxicity or material instability.

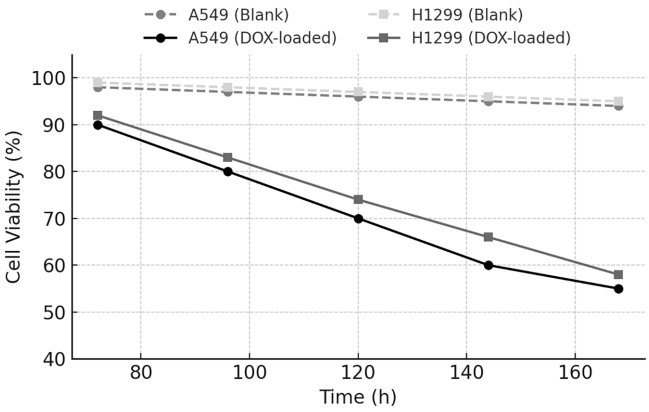

Figure 4. Long-term cytotoxicity of blank and DOX-loaded PLGA microspheres toward A549 and H1299 cells

As is shown in Figure 5, the antitumor effect of DOX-loaded PLGA microspheres was further evaluated in A549 3D tumor spheroids using live/dead staining. Spheroids treated with blank PLGA microspheres showed predominantly green fluorescence, indicating that most cells remained viable and that the blank carrier did not induce obvious cytotoxicity in the 3D model. In contrast, spheroids treated with DOX-loaded PLGA microspheres displayed extensive red fluorescence, particularly in the inner region of the spheroid, together with reduced green fluorescence at the periphery. These observations

indicate that sustained DOX release from the PLGA microspheres induced marked cell death in compact tumor spheroids. To determine whether oxidative stress was associated with this cytotoxic response, intracellular ROS levels were assessed using DCFH-DA staining. Blank PLGA microspheres produced only a minor change in ROS level compared with the control group (1.08 ± 0.10-fold vs. 1.00 ± 0.07-fold). Free DOX increased ROS accumulation to 1.74 ± 0.16-fold, whereas DOX-loaded PLGA microspheres further increased the ROS level to 2.46 ± 0.21-fold. When NAC was added, the ROS level in the DOX-loaded PLGA group decreased to 1.32 ± 0.12-fold. These results suggest that DOX-loaded PLGA microspheres enhanced intracellular ROS accumulation in A549 tumor spheroids, which was associated with the observed cytotoxic effect.

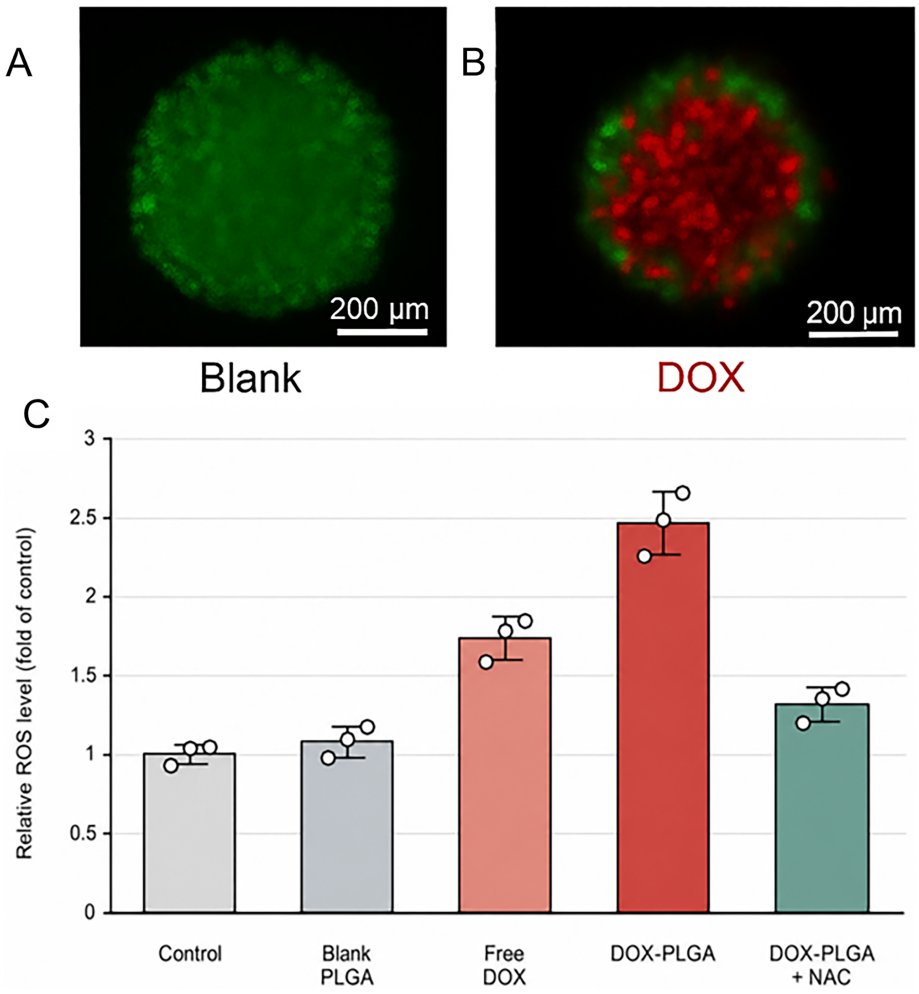

Figure 5. DOX-loaded PLGA microspheres enhance intracellular ROS accumulation and induce ROS-associated cytotoxicity in A549 3D tumor spheroids. (**A**) Live/dead staining and intracellular ROS generation in A549 3D tumor spheroids after treatment with DOX-loaded PLGA microspheres. (**B**) Representative live/dead fluorescence images of A549 tumor spheroids treated with blank PLGA microspheres or DOX-loaded PLGA microspheres. Live cells were stained green with Calcein-AM, whereas dead cells were stained red with EthD-1. Scale bar = 200 µm. (**C**) Quantification of intracellular ROS levels in A549 tumor spheroids after treatment with control medium, blank PLGA microspheres, free DOX, DOX-loaded PLGA microspheres, or DOX-loaded PLGA microspheres plus NAC. ROS levels were measured using DCFH-DA staining and normalized to the control group. Data are presented as mean ± SD (n = 3), with individual points representing independent replicates. DOX-PLGA, DOX-loaded PLGA microspheres; NAC, N-acetylcysteine

4. Discussion

Figure 1 serves as a conceptual guide that links material design principles with experimental evaluation, clarifying the scope and intent of the present work. PLGA undergoes hydrolytic degradation of its ester backbone, providing a basis for its use as a biodegradable drug carrier [9]. In the present study, incubation under oxidative conditions was used to examine environment-dependent changes in degradation and release; this is distinct from demonstrating selective ROS-triggered chemistry. The biological assessment comprises cytocompatibility and cytotoxicity testing in NSCLC cell models, with hemolysis testing as an additional compatibility assessment. These experiments provide preliminary *in vitro* evidence and do not establish efficacy or safety after implantation in a postoperative cavity. The 3D spheroid component of the schematic further emphasizes the biological challenge addressed by the study. Compared with 2D monolayer cultures, tumor spheroids provide a more restrictive environment for drug penetration [19]. Therefore, observing cytotoxicity in this model provides a preliminary indication that DOX delivery may affect compact tumor-like structures. However, Figure 1 should be interpreted as a conceptual summary rather than direct proof of every indicated pathway. The current evidence supports sustained DOX release and associated cytotoxicity in NSCLC models, while the relative contribution of oxidative stress requires further validation.

Figure 2 provides a comprehensive overview of the material properties of the PLGA microspheres, linking their morphology, size distribution, oxidative degradation behavior, and dispersion stability. Emulsion-based techniques are widely used to prepare PLGA microspheres, and formulation conditions influence their morphology and release characteristics [21]. The spherical morphology and limited aggregation observed by SEM indicate that the particles remained structurally intact during preparation. The relatively rough surface topology may facilitate water penetration into the polymer matrix, thereby influencing degradation and release behavior. The bimodal size distribution observed in DLS measurements may arise from the coexistence of individual particles and a fraction of loosely associated particles formed during emulsification; this explanation remains to be tested. Importantly, the dominant nanoscale population falls within a size range suitable for diffusion-based release and interaction with cells *in vitro*. The molecular weight retention study shows a faster Mw decrease in the tested oxidative medium. This observation is consistent with enhanced polymer degradation, although it does not identify a specific ROS-mediated bond-cleavage mechanism. Rather than indicating rapid structural failure, this behavior reflects a progressive degradation process that may underlie the controlled release characteristics of the system. Finally, the moderate increase in hydrodynamic diameter and PDI in serum-containing medium reflects partial protein adsorption and limited particle association, phenomena that are expected in complex biological fluids. The absence of drastic aggregation supports the suitability of the microspheres for short- to medium-term cell culture studies. Collectively, these results provide a material characterization basis for the subsequent biological evaluations and indicate environment-dependent behavior under the tested conditions.

The high encapsulation efficiency and consistent drug loading shown in Figure 3 support the suitability of PLGA microspheres as a carrier platform for incorporating small molecular payloads while maintaining formulation reproducibility. The release profiles indicate that the microspheres can maintain a controlled release pattern under physiological conditions, while exhibiting faster release in environments that more strongly promote polymer degradation. PLGA degradation and release behavior depend on the pH of the surrounding medium [9]. In the present study, release increased under mildly acidic and oxidative conditions, but the relative contributions of polymer degradation, drug diffusion, and matrix permeability were not resolved. Notably, the ROS-triggered acceleration appears as a progressive increase rather than an abrupt burst, which is important for interpreting the system as stimulus-responsive erosion/diffusion coupling rather than unstable encapsulation. Overall, these data provide material-level evidence that the microspheres can tune release kinetics in response to oxidative environments, forming the basis for subsequent evaluations focused on biosafety and cell compatibility. Initial burst release is a recognized feature of some PLGA formulations and depends on

the drug distribution and properties of the carrier [10]. In the present study, although an early release phase was detected, the release curve did not suggest a pronounced severe burst release within the tested time window, since drug elution continued progressively rather than reaching a near-maximum value immediately after exposure to the release medium. This behavior may be attributed to the fact that the encapsulated compound was not exclusively associated with the particle surface but remained at least partially distributed within the PLGA matrix, allowing release to proceed through a combination of diffusion and gradual polymer erosion. Previous work on double-walled PDLLA(PLGA) microspheres has shown that drug distribution and polymer structure affect release behavior [14]. Therefore, the release behavior observed here is more consistent with an early-stage release followed by sustained elution, rather than uncontrolled initial dumping.

The high cell viability in Figure 4 observed for blank microspheres suggests that the PLGA carrier itself is non-toxic and suitable for biomedical applications. The progressive decline in viability following DOX loading is consistent with continued exposure to released drug, although the viability assay alone does not determine the release mechanism. Sustained DOX release and antitumor activity have been reported for PLGA nanoparticles [22]. DOX delivered from acid-ended PLGA nanoparticles also retained cytotoxic activity against MDA-MB-231 cells [23]. These formulation-specific findings support the feasibility of retaining DOX activity after encapsulation, while the activity of the present formulation is supported by its own cell-viability results. The minimal hemolysis further indicates that the microspheres are hemocompatible and unlikely to induce adverse blood responses during local implantation. Together, these findings validate the safety and therapeutic potential of the PLGA microsphere system for local treatment-mimicking condition. The expanded biocompatibility assessment presented in Figure 4 provides important material-level evidence supporting the safe use of PLGA microspheres in biological environments. The sustained high viability observed for cells exposed to blank microsphere extracts confirms that the polymer carrier itself is intrinsically cytocompatible and that the fabrication process did not introduce harmful residues. This finding is particularly relevant for ROS-responsive systems, where oxidative conditions could potentially generate reactive degradation products. The absence of detectable toxicity in the blank group suggests that such byproducts, if present, are produced at levels insufficient to adversely affect cell viability. The time-dependent reduction in cell viability observed for payload-loaded microspheres should be interpreted in the context of controlled release behavior rather than direct material toxicity. The gradual decline over time, without an early-stage viability collapse, aligns well with the sustained release profiles described previously and indicates that cellular responses are governed by prolonged exposure to low concentrations of the released compound. This release-mediated effect contrasts with acute cytotoxicity typically associated with burst release or unstable encapsulation, underscoring the controlled nature of the PLGA matrix.

Hemocompatibility is an additional critical consideration for materials intended for potential contact with blood or vascularized tissues. The low hemolysis ratios observed for both blank and loaded microspheres indicate limited red blood cell membrane damage under the conditions of the present assay. The slightly higher hemolysis associated with the loaded microspheres may be related to the payload, but this experiment does not establish *in vivo* blood compatibility or a clinical safety threshold. Taken together, these results indicate that the PLGA microspheres exhibit favorable cytocompatibility and hemocompatibility profiles, supporting their use as a stable and biologically acceptable carrier platform for further ROS-responsive material studies rather than implying direct therapeutic efficacy. The live/dead staining results confirm the strong cytotoxic effect of sustained DOX release on 3D tumor spheroids. The increased red fluorescence within DOX-treated spheroids indicates cell death in the imaged regions; live/dead staining alone does not quantify drug penetration or distinguish apoptosis from necrosis. This spatial distribution of cell death contrasts with the uniformly viable blank control, demonstrating that the cytotoxic response arises from the released drug rather than the microsphere carrier. The outcome is consistent with the long-term viability assay and supports cytotoxic activity in 3D culture. Baek et al. reported spheroid shrinkage with sustained dual-drug

delivery from hollow PLGA microparticles in MCF-7 spheroids [20]. That finding provides a precedent for evaluating drug-releasing PLGA systems in 3D culture, but it does not establish drug distribution or apoptosis in the present NSCLC spheroids. Results in Figure 5 provide an *in vitro* assessment of tumor-cell responses rather than validation of postoperative residual tumor control. The live/dead staining results demonstrate that the PLGA carrier itself was well tolerated in the 3D spheroid model, whereas DOX-loaded PLGA microspheres induced substantial tumor-cell death. This finding is consistent with the sustained release behavior of the microsphere formulation and supports the use of PLGA microspheres as a local DOX delivery platform for treatment-mimicking conditions. The ROS results provide additional mechanistic support for the cytotoxicity observed in the spheroids. Compared with free DOX, DOX-loaded PLGA microspheres produced a higher ROS signal, which may reflect prolonged DOX exposure enabled by sustained release from the polymer matrix. The reduction of ROS accumulation after NAC treatment further indicates that oxidative stress was involved in the cellular response. However, the relative contribution of ROS to cell death remains unresolved. DOX can cause DNA damage through topoisomerase II-mediated processes [24]. DNA intercalation and activation of apoptosis-related pathways are also established components of DOX pharmacology [25]. These literature-based mechanisms provide context and were not directly measured in the present study. Therefore, the present results support an association between DOX-PLGA treatment, increased ROS accumulation, and cytotoxicity in 3D NSCLC spheroids. As a result, enhanced cell death is observed in the spheroid core, as indicated by the increased red fluorescence in live/dead staining. Taken together, these results suggest that the observed cytotoxicity arises from a combination of controlled release kinetics and well-established intracellular mechanisms of DOX, rather than from abrupt or uncontrolled material degradation.

5. Conclusion

In summary, DOX-loaded PLGA microspheres were successfully developed as a biodegradable platform for localized and sustained drug delivery. The microspheres exhibited well-defined morphology, acceptable size distribution, stable drug encapsulation, and environment-dependent release behavior, together with favorable cytocompatibility of the blank carrier and sustained inhibitory effects of the loaded formulation in 2D and 3D *in vitro* models. These results support the feasibility of using PLGA microspheres as a material platform for local treatment-mimicking condition. Nevertheless, several limitations should be acknowledged. The current study is limited to *in vitro* evaluation and does not yet provide evidence from *in vivo* models. In addition, the release behavior and material stability should be further investigated under more complex physiological conditions to better approximate the postoperative microenvironment. Future work should therefore focus on validating the long-term biosafety, degradation behavior, and therapeutic performance of this system in more clinically relevant settings, as well as optimizing the formulation to achieve more precise and controllable local drug delivery.

Acknowledgement: The authors acknowledge the use of DeepSeek for English language polishing during manuscript preparation.

Funding Statement: The authors received no specific funding for this study.

Author Contributions: All authors contributed to this present work: Lin Shen designed the study, developed the methodology, performed the experiments, analyzed the data, and drafted and revised the manuscript. Fanzhi Men performed the experiments and acquired the data. Changchang Hu and Bin Qiao interpreted the data and provided supervision and critical revisions. All authors reviewed and approved the final version of the manuscript.

Availability of Data and Materials: The datasets generated and/or analyzed during the current study are available from the corresponding author Lin Shen upon reasonable request.

CC BY

Ethics Approval: Ethical approval was not required for this study because it is not involved any human experiments.

Conflicts of Interest: Lin Shen and Changchang Hu are employees of Anhui Nutrition Biotechnology Co., Ltd. The company provided no funding, materials, or other resources for this study, and had no role in the study design, data collection, analysis, or manuscript preparation. The remaining authors declare no competing interests.

Abbreviations

PLGA	Poly(lactic-co-glycolic acid)
NSCLC	Non-small cell lung cancer
FDA	Food and drug administration
PVA	Poly(vinyl alcohol)
DOX·HCl	Doxorubicin hydrochloride
DCM	Dichloromethane
DMSO	Dimethyl sulfoxide
PBS	Phosphate-buffered saline
EthD-1	Ethidium homodimer-1
FBS	Fetal bovine serum
W/O/W	Water-in-oil-in-water
SEM	Scanning electron microscopy
PDI	Polydispersity index
DLS	Dynamic light scattering
RBCs	Red blood cells

References

1. Hendriks LEL, Remon J, Faivre-Finn C, Garassino MC, Heymach JV, Kerr KM, et al. Non-small-cell lung cancer. Nat Rev Dis Primers. 2024;10(1):71. doi:10.1038/s41572-024-00551-9.
2. Bray F, Laversanne M, Sung H, Ferlay J, Siegel RL, Soerjomataram I, et al. Global cancer statistics 2022: GLOBOCAN estimates of incidence and mortality worldwide for 36 cancers in 185 countries. CA Cancer J Clin. 2024;74(3):229–63. doi:10.3322/caac.21834.
3. Predina JD, Keating J, Patel N, Nims S, Singhal S. Clinical implications of positive margins following non-small cell lung cancer surgery. J Surg Oncol. 2016;113(3):264–9. doi:10.1002/jso.24130.
4. Wong LY, Dale R, Kapula N, Elliott IA, Liou DZ, Backhus LM, et al. Impacts of positive margins and surgical extent on outcomes after early-stage lung cancer resection. Ann Thorac Surg. 2024;118(5):1126–34. doi:10.1016/j.athoracsur.2024.05.032.
5. Winton T, Livingston R, Johnson D, Rigas J, Johnston M, Butts C, et al. Vinorelbine plus cisplatin vs. observation in resected non-small-cell lung cancer. N Engl J Med. 2005;352(25):2589–97. doi:10.1056/NEJMoa043623.
6. Liu R, Wolinsky JB, Walpole J, Southard E, Chirieac LR, Grinstaff MW, et al. Prevention of local tumor recurrence following surgery using low-dose chemotherapeutic polymer films. Ann Surg Oncol. 2010;17(4):1203–13. doi:10.1245/s10434-009-0856-z.
7. Azouz SM, Walpole J, Amirifeli S, Taylor KN, Grinstaff MW, Colson YL. Prevention of local tumor growth with paclitaxel-loaded microspheres. J Thorac Cardiovasc Surg. 2008;135(5):1014–21. doi:10.1016/j.jtcvs.2007.12.011.

8. Jusu SM, Obayemi JD, Salifu AA, Nwazojie CC, Uzonwanne V, Odusanya OS, et al. Drug-encapsulated blend of PLGA-PEG microspheres: *in vitro* and *in vivo* study of the effects of localized/targeted drug delivery on the treatment of triple-negative breast cancer. Sci Rep. 2020;10(1):14188. doi:10.1038/s41598-020-71129-0.
9. Makadia HK, Siegel SJ. Poly lactic-co-glycolic acid (PLGA) as biodegradable controlled drug delivery carrier. Polymers. 2011;3(3):1377–97. doi:10.3390/polym3031377.
10. Siepmann J, Siepmann F. Release mechanisms of PLGA-based drug delivery systems: a review. Int J Pharm X. 2025;10(15):100440. doi:10.1016/j.ijpx.2025.100440.
11. Lin R, Shi Ng L, Wang CH. *In vitro* study of anticancer drug doxorubicin in PLGA-based microparticles. Biomaterials. 2005;26(21):4476–85. doi:10.1016/j.biomaterials.2004.11.014.
12. Hsu MY, Huang YT, Weng CJ, Chen CM, Su YF, Chu SY, et al. Preparation and *in vitro*/*in vivo* evaluation of doxorubicin-loaded poly [lactic-co-glycol acid] microspheres using electrospray method for sustained drug delivery and potential intratumoral injection. Colloids Surf B Biointerfaces. 2020;190:110937. doi:10.1016/j.colsurfb.2020.110937.
13. Gu B, Sun X, Papadimitrakopoulos F, Burgess DJ. Seeing is believing, PLGA microsphere degradation revealed in PLGA microsphere/PVA hydrogel composites. J Control Release. 2016;228:170–8. doi:10.1016/j.jconrel.2016.03.011.
14. Xu Q, Chin SE, Wang CH, Pack DW. Mechanism of drug release from double-walled PDLLA(PLGA) microspheres. Biomaterials. 2013;34(15):3902–11. doi:10.1016/j.biomaterials.2013.02.015.
15. Mensah RA, Kirton SB, Cook MT, Styliari ID, Hutter V, Chau DYS. Optimising poly(lactic-co-glycolic acid) microparticle fabrication using a Taguchi orthogonal array design-of-experiment approach. PLoS One. 2019;14(9):e0222858. doi:10.1371/journal.pone.0222858.
16. Paliashvili K, Popov A, Kalber TL, Patrick PS, Hayes A, Henley A, et al. Peritumoral delivery of docetaxel-TIPS microparticles for prostate cancer adjuvant therapy. Adv Ther. 2021;4(2):2000179. doi:10.1002/adtp.202000179.
17. Zhan Y, Du YT, Yang ZZ, Zhang CL, Qi XR. Preparation and characterization of paclitaxel microspheres *in situ* gel and its antitumor efficacy by local injection. J Peking Univ. 2019;51(3):477–86. doi:10.19723/j.issn.1671-167X.2019.03.015.
18. Liu J, Meisner D, Kwong E, Wu XY, Johnston MR. Translymphatic chemotherapy by intrapleural placement of gelatin sponge containing biodegradable Paclitaxel colloids controls lymphatic metastasis in lung cancer. Cancer Res. 2009;69(3):1174–81. doi:10.1158/0008-5472.CAN-08-1753.
19. Mehta G, Hsiao AY, Ingram M, Luker GD, Takayama S. Opportunities and challenges for use of tumor spheroids as models to test drug delivery and efficacy. J Control Release. 2012;164(2):192–204. doi:10.1016/j.jconrel.2012.04.045.
20. Baek JS, Choo CC, Tan NS, Loo SCJ. Sustained-releasing hollow microparticles with dual-anticancer drugs elicit greater shrinkage of tumor spheroids. Oncotarget. 2017;8(46):80841–52. doi:10.18632/oncotarget.20591.
21. Su Y, Zhang B, Sun R, Liu W, Zhu Q, Zhang X, et al. PLGA-based biodegradable microspheres in drug delivery: recent advances in research and application. Drug Deliv. 2021;28(1):1397–418. doi:10.1080/10717544.2021.1938756.
22. Kim J, Choi Y, Yang S, Lee J, Choi J, Moon Y, et al. Sustained and long-term release of doxorubicin from PLGA nanoparticles for eliciting anti-tumor immune responses. Pharmaceutics. 2022;14(3):474. doi:10.3390/pharmaceutics14030474.
23. Betancourt T, Brown B, Brannon-Peppas L. Doxorubicin-loaded PLGA nanoparticles by nanoprecipitation: preparation, characterization and *in vitro* evaluation. Nanomedicine. 2007;2(2):219–32. doi:10.2217/17435889.2.2.219.

24. Tewey KM, Rowe TC, Yang L, Halligan BD, Liu LF. Adriamycin-induced DNA damage mediated by mammalian DNA topoisomerase II. Science. 1984;226(4673):466–8. doi:10.1126/science.6093249.
25. Thorn CF, Oshiro C, Marsh S, Hernandez-Boussard T, McLeod H, Klein TE, et al. Doxorubicin pathways: pharmacodynamics and adverse effects. Pharmacogenet Genom. 2011;21(7):440–6. doi:10.1097/FPC.0b013e32833ffb56.

Received: 08 January 2026; Accepted: 04 June 2026; Published: XX XX 2026